PAPER

Check for updates

Novel anti-hyperuricemic hexapeptides derived from *Apostichopus japonicus* hydrolysate and their modulation effects on the gut microbiota and host microRNA profile†

Siqing Fan,‡[a,b] Yumeng Huang,‡[a,c] Guoding Lu,[d] Na Sun,[d] Rui Wang,[b] Chenyang Lu, ID *[a,c] Lijian Ding,[b] Jiaojiao Han,[a,c] Jun Zhou,[a,c] Ye Li, ID [a,c] Tinghong Ming*[a,c] and Xiurong Su[a,c]

Hyperuricemia (HUA) is the second most common metabolic disease nowadays, and is characterized by permanently increased concentrations of serum uric acid. In this study, two novel hexapeptides (GPAGPR and GPSGRP) were identified from *Apostichopus japonicus* hydrolysate and predicted to have xanthine oxidase (XOD) inhibitory activity by molecular docking. Their *in vitro* XOD inhibition rates reached 37.3% and 48.6%, respectively, at a concentration of 40 mg mL^{-1}. Subsequently, *in vivo* experiments were carried out in a HUA mouse model, and we found that both peptides reduced the serum uric acid by inhibiting uric acid biosynthesis and reabsorption, as well as alleviated renal inflammation *via* suppressing the activation of the NLRP3 inflammasome. 16S rDNA sequencing indicated that both peptide treatments reduced the richness and diversity of the gut microbiota, altered the composition in the phylum and genus levels, but different change trends were observed in the phylum Verrucomicrobia and genera *Akkermansia*, *Dubosiella*, *Alloprevotella*, Clostridium unclassified and *Alistipes*. In addition, changes in the renal microRNA (miRNA) profiles induced by GPSGRP treatment were analyzed; 21 differentially expressed (DE) miRNAs were identified among groups, and KEGG pathway analysis indicated that their potential target genes were involved in pluripotency of stem cell regulation, mTOR signaling pathway and proteoglycans. Moreover, ten miRNAs involved in the HUA onset and alleviation were identified, which showed a high correlation with genera related to the metabolism of short-chain fatty acids, bile acids and tryptophan. This study delineated two hexapeptides as potential microbiota modulators and miRNA regulators that can ameliorate HUA.

Introduction

Hyperuricemia (HUA) is a progressive metabolic condition caused by permanently increased concentrations of serum uric acid and has gradually become the second most common metabolic disease after type 2 diabetes.[1] Uric acid is mainly synthesized in the liver, and xanthine oxidase (XOD), one of the rate-limiting enzymes which is widely used as a HUA man-

[a]State Key Laboratory for Managing Biotic and Chemical Threats to the Quality and Safety of Agro-products, Ningbo University, Ningbo, China.
E-mail: luchenyang@nbu.edu.cn
[b]College of Food and Pharmaceutical Sciences, Ningbo University, Ningbo, China
[c]School of Marine Science, Ningbo University, Ningbo, China
[d]Ningbo Green-Health Pharmaceutical Co., Ltd, Ningbo, China
†Electronic supplementary information (ESI) available. See DOI: 10.1039/d1fo03981d
‡These authors contributed equally to this work.

agement target, catalyzes hypoxanthine to xanthine and then to uric acid.[2] In addition, uric acid is excreted mainly *via* the kidneys mediated by reabsorption (GLUT9, URAT1, *etc.*) and secretion (MRP4, ABCG2, *etc.*).[3] The overactive uric acid production in the liver that exceeds uric acid excretion by the kidneys and intestinal tract contributes to HUA, and long-term high uric acid levels and uric acid crystal deposition exacerbate oxidative stress, up-regulate the TLR4/MyD88/NF-κB signaling pathway to generate pro-IL-1β, and activate the NLRP3 inflammasome for the cleavage of IL-1β from pro-IL-1β, and subsequently leads to renal inflammation and injury.[4] Moreover, HUA will increase the incidence of related diseases, including gout, kidney diseases, metabolic syndromes and cardiovascular disease.[5] Due to the inefficiency of nonpharmacological therapies, such as diet management, in reducing uric acid in patients, pharmacological therapies are needed. There are three main categories of uric acid management drugs: uric acid production inhibitors (allopurinol and febuxostat),

excretion promoters (probenecid and benzbromarone) and recombinant uricase (pegloticase). The first category is recommended as the first-line treatment for HUA in many countries, but various adverse effects have still been reported.[6]

As previously reported, *Apostichopus japonicus* oligopeptide (AJOP), prepared with an edible protein, is a safer alternative that exerts anti-HUA effects by rebalancing uric acid metabolism and inhibiting the NLRP3 inflammasome and NF-κB signaling pathway activation.[3,7] The various components and their multiple targets not only contribute to the comprehensive anti-HUA effects of AJOP but also hinder the further development of AJOP due to the unclear understanding of key peptides with anti-HUA effects. The purify-and-identify method has been widely used to screen peptides with distinct functions and structures *via* iterative rounds, but this method is one-sided, labor intensive and time-consuming.[8] In a previous study of AJOP, *in silico* molecular docking instead of the purify-and-identify method was used to predict the XOD inhibition activity of the identified peptides with high abundance,[7] but the anti-HUA effects and underlying mechanism of certain peptides need to be further explored both *in vitro* and *in vivo*.

The gut microbiota has become a potential target for understanding the onset and alleviation of HUA due to the correlation and causation relationship between them. Firstly, the absence of the gut microbiota in germ-free mice or after antibiotic treatment decreased joint inflammation induced by monosodium urate monohydrate crystal injection.[9] Then, modulated gut microbiota composition and metabolism were observed in hyperuricemic individuals.[10,11] In addition, the contributions of gut microbiota manipulations (probiotic and prebiotic) to HUA and renal inflammation alleviation have been reported by various studies,[12,13] and the anti-hyperuricemic effects of AJOP were transferable *via* fecal microbiota transplantation.[7] What's more, the microbiota produces thousands of diffusible metabolites, and the metabolites are reported to alleviate HUA by regulating the intestinal epithelial cell proliferation, ameliorating purine metabolism disorders, promoting uric acid excretion, and reducing inflammation.[14] However, the underlying mechanism by which the microbiota remotely regulates the functions of central metabolic organs, such as the liver and kidneys, is largely undetermined.

MicroRNAs (miRNAs) are small (19–23 nt) and single-stranded noncoding RNA molecules that were once considered redundant; however, accumulating studies have shown the specific and global regulatory effects of miRNAs on individual genes and regulatory networks. As previously reported, miRNAs are differentially expressed in the renal tissues of HUA and healthy individuals,[15] and several highly conserved miRNAs have been identified to be involved in the regulation of uric acid biosynthesis (miR-448, *etc*.), secretion (miR-34a, miR-143-3p, *etc*.), and immune response (miR-223, *etc*.);[16–18] thus we proposed that miRNAs play critical roles in the control of HUA development. In addition, miRNAs were reported to be regulated by the metabolites produced by the gut microbiota, including short-chain fatty acids (SCFAs), tryptophan derivatives and bile acids (BAs).[19–21] However, the modulation of miRNA profiles in HUA mice by treatment with distinct structural peptides remains unclear.

Herein, two peptides GPAGPR and GPSGRP were identified from *Apostichopus japonicus* hydrolysate and predicted to have XOD inhibitory activity by molecular docking. The anti-HUA effects of these two peptides were confirmed *in vitro* (XOD inhibition rate) and *in vivo* (HUA mice), and their modulation effects on the gut microbiota and host renal miRNA profile were explored.

Materials and methods

AJOP preparation and composition detection

Apostichopus japonicus (*A. japonicus*) was purchased from the Lulin Seafood Market (Ningbo, Zhejiang, China), and AJOP was prepared with 3% trypsin and alkaline protease in a ratio of 2 : 1 at 55 °C for 4 h as previously described.[7] Then, the enzyme was inactivated, and the supernatant was ultrafiltered with a 1000 Da membrane (Millipore, Burlington, MA, USA) and freeze dried using a vacuum freeze-drying machine (LABCONCO Co., Ltd, Kansas City, MO, USA). Subsequently, the composition and abundance of peptides in AJOP were measured by MALDI-TOF/TOF (Applied Biosystems, Foster City, CA, USA).

Prediction of XOD inhibitory activity by molecular docking

The thirteen major peptides (abundance >1%) detected by MALDI-TOF/TOF in this study were used as ligands in molecular docking studies to predict the *in silico* XOD inhibitory activity (Discovery Studio 2017, Beijing Chong Teng Technology Co., Ltd, Beijing, China), and the crystal structure of bovine milk XOD (PDB ID: 1FIQ) was obtained from the RCSB Protein Data Bank (http://www.rcsb.org/pdb) as the receptor. The CDOCKER program was used with the default parameters. The interaction between the ligand and receptor was characterized by -CDOCKER interaction energy (-CIE), and the highest -CIE value indicated the strongest interaction.

Measurement of XOD inhibitory activity *in vitro*

The peptides GPAGPR and GPSGRP were synthesized by Shanghai Mujin Biotech Co., Ltd (Shanghai, China) and dissolved in 50 mM Tris-HCl buffer at pH 7.5. First, 40 μL of XOD solution (0.05 U mL^{-1}) and 40 μL of peptide solutions (ranging from 10 to 60 mg mL^{-1}) or allopurinol solutions (ranging from 3 to 18 μg mL^{-1}) were mixed at 25 °C for 10 min. Subsequently, the reaction was started by adding 120 μL of xanthine solution (0.4 mM) into the mixture, the mixture was incubated at 25 °C, and the absorbance was measured at 290 nm every 30 s up to 25 min. Three replicates were set for each sample.

At the end of the experiment, the reaction was terminated by adding 64 μL of HCl (1 M), and the production of uric acid was measured by HPLC (Agilent 1200 series, Agilent Technologies Inc., CA, USA) with an Agilent ZORBAX Eclipse XDB-Phenyl column (250 × 4.6 mm i.d., 5 μm, Santa Clara, CA,

USA) as previously described.[22] The mobile phase was composed of water with sodium 1-pentane sulfonate (0.52 mM) and monopotassium phosphate (0.20 M) (pH 4.0, solvent A) and acetonitrile (solvent B) in a ratio of 85 : 15 (v/v). The detection wavelength was 290 nm and the flow rate was 1.0 mL min^{-1} at room temperature. The percentage of inhibition rate was calculated as follows: XOD inhibition rate (%) = [1 − (sample reaction UA production/control reaction UA production)] × 100%.

Animal experiment

The present study, referring to the laboratory animal care, was approved by the Ethical Committee of Experimental Animal Care at Ningbo University under permit no. 10525.

Twenty male C57BL/6 mice (five week old, 22.44 ± 1.37 g) purchased from Zhejiang Laboratory Animal Center (Hangzhou, Zhejiang, China) were housed in a specific pathogen free (SPF) room (23–25 °C, 60–80% relative humidity and a 12 h light/12 h dark cycle) with free access to water and food. After one week of acclimatization, twenty mice were randomly divided into four groups, namely, the control, model, GPAGPR and GPSGRP groups, with 5 mice per group. At 9 : 00, the mice in the control group received 200 μL of saline by oral gavage, and the mice in the remaining three other groups received 200 μL of HUA solution (containing 200 mg kg^{-1} d^{-1} of hypoxanthine, 30 mg kg^{-1} d^{-1} of yeast extract and 250 mg kg^{-1} d^{-1} of potassium oxonate) every day for 12 weeks as previously described.[23] At 15 : 00, the mice in the peptide groups were administered 200 μL of GPAGPR or GPSGRP (10 mg kg^{-1} d^{-1}) by oral gavage for 12 weeks, while the mice in the control and model groups were administered 200 μL of saline by oral gavage. The dosages of GPAGPR and GPSGRP were selected according to the previous results reported by our group[8] and are equivalent to 49.8 mg d^{-1} in humans.[24]

At the end of 12 weeks, urine was collected from each mouse and stored at −80 °C. After anaesthetizing the animals, the serum was separated, and the liver, kidney and cecal contents were collected and stored at −80 °C for further analysis. The uric acid and blood urea nitrogen (BUN) in the serum and urine were quantified using commercial kits (No. C012-2-1 and C013-2-1) purchased from Nanjing Jiancheng Co., Ltd (Nanjing, Jiangsu, China).

Measurement of mRNA and protein expression

mRNA and protein expressions were measured by qRT-PCR and western blot analysis. For qRT-PCR, total RNA was extracted from the liver and kidneys using the TransZol Up Plus RNA kit (TransGen Biotech, Beijing, China), and cDNA was synthesized using mRNA as a template with TransScript® All-in-One First-Strand cDNA Synthesis SuperMix (TransGen Biotech, Beijing, China). mRNA levels were measured with the primers described in Table S1† using an ABI 7500 Real Time Detection System (Applied Biosystems, Bedford, MA, USA) following the default program in a 20 μL reaction volume. Three replicates were set for each sample, and the mRNA level was normalized to the β-actin level and calculated using the 2$^{-\Delta\Delta CT}$ method.

As previously reported,[25] the liver and kidneys were lysed in RIPA buffer (Sangon Biotech Co., Ltd, Shanghai, China), the homogenate was centrifuged at 13 000g for 15 min, the supernatant was collected as total protein, and the protein concentration was measured via a BCA protein assay kit (Beijing ComWin Biotech Co., Ltd, Beijing, China) according to the manufacturer's protocol. Denatured proteins were separated by SDS-PAGE and transferred to polyvinylidene fluoride membranes (Millipore Corp, Billerica, MA, USA). Nonspecific binding to the membranes was blocked with 5% nonfat milk powder for 1 h at room temperature, incubated overnight with primary antibodies against Glut9 (1 : 800, D162759, 54 kDa), ADA (1 : 700, D221495, 41 kDa), ABCG2 (1 : 500, D155255, 72 kDa), IL-1β (1 : 1000, #63124, 17 kDA), ASC (1 : 800, #67824, 22 kDa), cleaved caspase-1 (1 : 900, #89332, 22 kDa) and caspase-1 (1 : 1000, #24232, 48 kDa) at 4 °C, and then with horseradish peroxidase-conjugated secondary antibodies for 1 h at room temperature. The first three primary antibodies were purchased from Sangon Biotech Co., Ltd (Shanghai, China) and the rest were purchased from Cell Signaling Technology (Shanghai, China). Finally, the bands were visualized using an ECL kit (Advansta Inc, San Jose, CA, USA) with a ChemiDoc XRS+ Imaging System (Bio-Rad Laboratories Inc, Hercules, CA, USA).

16S rDNA amplicon sequencing and data analysis

As previously reported,[26] total bacterial genomic DNA was extracted from the cecal contents with an E.Z.N.A.® Stool DNA kit (Omega, Norcross, GA, USA) and quantified with a NanoDrop 2000c spectrophotometer (Thermo-Fisher Scientific, Waltham, MA, USA). The V3–V4 region of 16S rDNA was amplified with barcoded primers 319F (5′-ACTCCTACGGG-AGGCAGCAG-3′) and 806R (5′-GGACTACHVGGGTWTCTAAT-3′) with the default program in a 25 μL reaction volume, containing 12.5 μL of Premix Ex Taq™ Hot Start Version (Takara Biotechnology Co. Ltd, Dalian, China), 0.1 μM each primer, and 20 ng of template. Amplification was initiated at 98 °C for 30 s, followed by 35 cycles of denaturation at 98 °C for 10 s, primer annealing at 54 °C for 30 s, extension at 72 °C for 45 s, and final extension for 10 min. The presence of amplicons was confirmed by gel electrophoresis, and the purified PCR products were used to prepare a PCR product library. Subsequently, the amplicon sequencing was performed in LC-Bio (Hangzhou, Zhejiang, China) with an Illumina MiSeq platform (Illumina, San Diego, CA, USA) using 2 × 300 bp PE sequencing and multiple sequencing runs. The raw data were filtered via QIIME 2 (https://qiime2.org/) and classified with the RDP database. In addition, α diversity analysis was calculated using Mothur,[27] and β diversity analysis was calculated using QIIME2. The differentially abundant genera were identified via the Kruskal–Wallis test. Spearman's correlation analysis between the abundance of differentially abundant genera and phenotypes of HUA was calculated using SPSS (version

19.0, Chicago, IL, USA), and correlations were defined as significant when $p < 0.05$ and FDR < 0.25.

miRNA profile sequencing and analysis

Total RNA was extracted from the kidneys using a commercial kit following the manufacturer's recommendations, and the concentration and quality of total RNA were detected using a NanoDrop 2000c spectrophotometer. The RNA was purified using 15% agarose gels and enriched by ethanol precipitation. A TruSeq Small RNA Sample Prep kit (Illumina, San Diego, CA, USA) was used to construct the library, which was subsequently sequenced using the Illumina HiSeq 2000/2500 platform at 1×50 bp.

Raw reads were submitted to ACGT101-miR (LC Sciences, Houston, TX, USA) to remove adapter dimers, junk, low complexity sequences, common RNA families and repeats. Subsequently, known and novel miRNAs were identified by mapping the unique sequences (19–26 nt) to specific species precursors in miRbase (version 22.0) using BLAST. In this study, differentially expressed (DE) miRNAs between two groups based on normalized deep-sequencing counts were analyzed using Student's t test, while DE-miRNAs among the three groups were analyzed using ANOVA, and the significance threshold was set to 0.05. In addition, both TargetScan (version 5.0) and Miranda (version 3.3a) were used to predict the target genes of certain DE-miRNAs, and the overlapping genes predicted by both software programs were used for further analysis. Moreover, the target genes were annotated by GO and KEGG pathway analyses.

Statistical analysis

All data are presented as mean ± standard deviation (SD). The differences among groups were calculated by one-way analysis of variance (ANOVA) followed by Tukey's *post hoc* tests *via* MATLAB R2012a (MathWorks, Natick, MA, USA), and $p < 0.05$ was defined as the statistical significance.

Accession number

The sequences have been deposited in the Read Archive Database under PRJNA752999 (16S rDNA sequencing) and PRJNA753202 (miRNA sequencing).

Results

Potential interactions between XOD and the major peptides in AJOP

The peptide profiles in AJOP were measured by MALDI-TOF/TOF-MS as previously described,[7] and 13 peptides with relatively high abundance (>1%) were identified (Table S2†). Subsequently, the potential interactions between XOD and peptides were predicted *via* molecular docking, and two hexapeptides with similar structures, GPAGPR and GPSGRP, showed high binding ability with XOD characterized by lower CIE (Fig. 1A, B and Table S3†). Therefore, these two similar

peptides were predicted to have XOD inhibitory activities and are involved in HUA alleviation.

Inhibitory effects of GPAGPR and GPSGRP on XOD activity *in vitro*

The peptides GPAGPR and GPSGRP were synthesized, and their inhibitory activities on XOD were subsequently measured and compared *in vitro*, and allopurinol (an XOD inhibitor used in clinic) was used as the positive control. The production of uric acid gradually increased in the presence of both peptides at all assessed concentrations from 0 to 25 min (Fig. 1C and E). The inhibition rate of XOD reached 41.2% in the presence of allopurinol at a concentration of 3 μg mL^{-1} (Fig. S1†), while GPAGPR and GPSGRP showed similar inhibition rates (37.3% and 48.6%) at a concentration of 40 mg mL^{-1} (Fig. 1D and F). This experiment confirmed the XOD inhibitory activities of GPAGPR and GPSGRP *in vitro*, even though they are relatively far lower than that of allopurinol. Then, we investigated their anti-HUA effects *in vivo via* a high-purine-diet (HPD)-induced HUA mouse model.

GPAGPR and GPSGRP treatments attenuated HUA in mice

The body weights of mice in all groups gradually increased during the 12-week experiment. Both peptides significantly restored the increased body weight gain induced by the HPD treatment ($p < 0.01$), but relatively lower body weight gain was observed in the GPSGRP group (Fig. S2†). In addition, treatment with both peptides attenuated the phenotypes of HUA in mice, characterized by reduced uric acid ($p < 0.01$) and urea nitrogen in serum ($p < 0.01$) (Fig. 2A and B), and enhanced uric acid in the urine ($p < 0.01$) (Fig. 2C), and no significant difference was observed between the GPAGPR and GPSGRP groups. Moreover, neither HPD nor peptide treatments affected the urea nitrogen level of urine (Fig. 2D).

GPAGPR and GPSGRP treatments rebalanced uric acid metabolism in HUA mice

As expected, the mRNA level of XOD induced by HPD in the liver was significantly downregulated by the treatment with peptides ($p < 0.001$ and $p < 0.01$), while ADA, another key enzyme involved in the uric acid biosynthesis, was upregulated by GPAGPR ($p > 0.05$) and downregulated by GPSGRP ($p < 0.05$) in both mRNA and protein levels (Fig. 3A and B). In addition, the peptides inhibited uric acid reabsorption and secretion in the kidneys by the corresponding regulation of GLUT9 ($p < 0.01$) and ABCG2 ($p < 0.05$ and $p < 0.01$) at the mRNA and protein levels, respectively, but showed no significant effects on URAT1 and MRP4 (Fig. 3C–F).

GPAGPR and GPSGRP treatments regulated cytokine release in HUA mice

Long-term high uric acid in serum will lead to potential inflammation of the kidneys. Therefore, the mRNA and protein levels of the representative inflammatory cytokines, including IL-1β, TNF-α and IL-10, in the kidneys were measured by qRT-PCR and western blot analysis. Both pep-
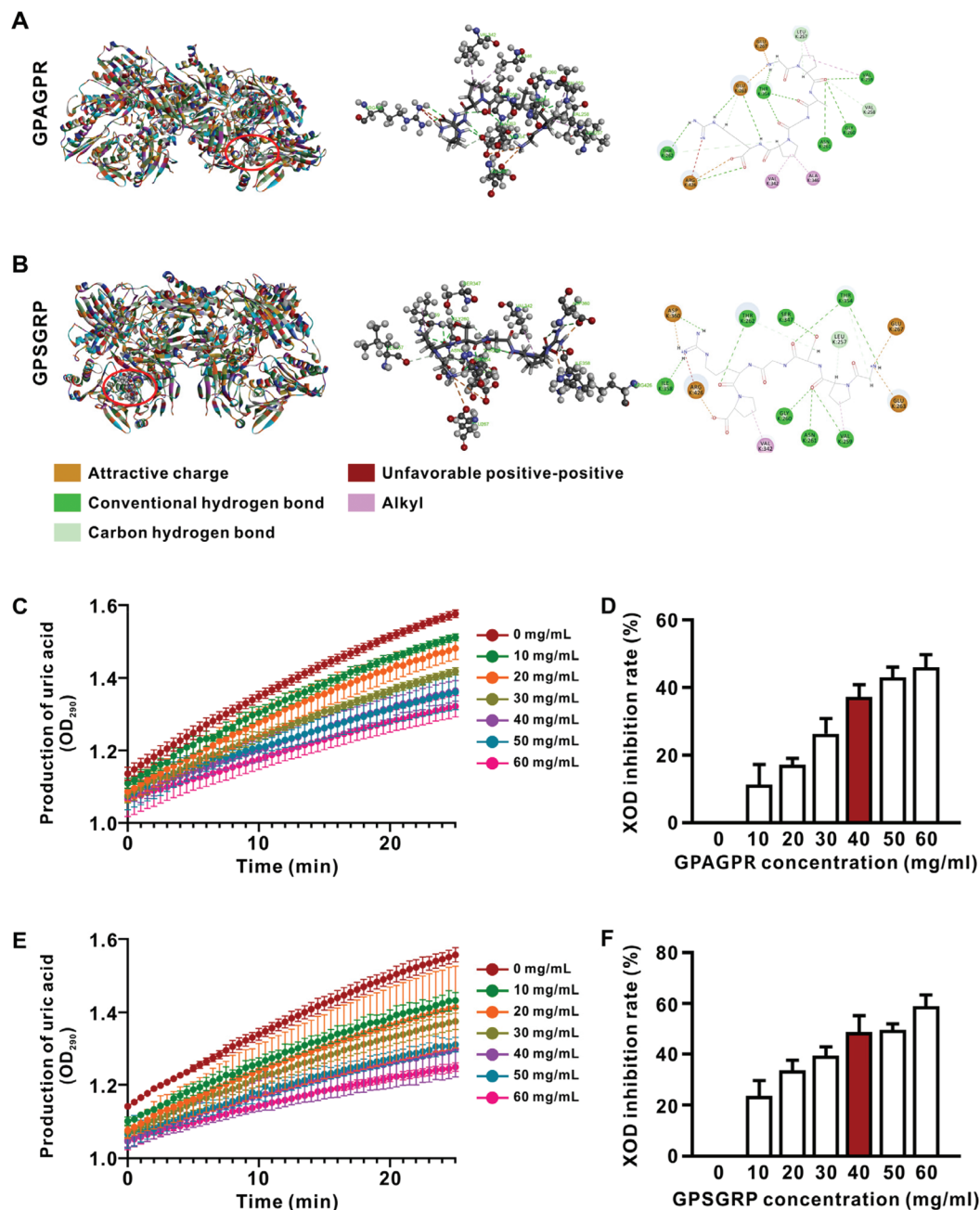
Fig. 1 Visualization of molecular docking and *in vitro* XOD inhibitory rate between the peptides and XOD. A. GPAGPR-XOD. B. GPSGRP-XOD. Effects of different concentrations of GPAGPR (C) and GPSGRP (E) on uric acid production over 25 min. Final XOD inhibition rates of GPAGPR (D) and GPSGRP (F) at different concentrations. Data are shown as mean $\pm$ SD, $n = 3$.

tides significantly reduced the mRNA and protein levels of IL-1β ($p < 0.01$ and $p < 0.001$). GPSGRP significantly downregulated the mRNA level of TNF-α ($p < 0.05$), and GPAGPR treatment further aggravated the enhanced mRNA level of TNF-α induced by HPD ($p > 0.05$), although not reaching a significant level. In addition, neither HPD nor peptide significantly affected IL-10 at the mRNA level ($p > 0.05$) (Fig. 4A and B).

Considering the important roles of the NLRP3 inflammasome and TLR4/MyD88/NF-κB pathway in the release of cytokines, particularly IL-1β, the expression levels and activation of

related proteins were measured. As expected, NLRP3 inflammasome activation was induced by HPD, characterized by enhanced NLRP3 ($p < 0.01$), ASC ($p < 0.001$) and caspase-1 ($p < 0.05$) in mRNA levels, and this activation was significantly inhibited by both peptides (Fig. 4C). In addition, the ratio of cleaved caspase-1 (c-caspase-1) to total caspase-1 (t-caspase-1) was decreased by the peptide treatments (Fig. 4D). Otherwise, neither HPD nor the peptide treatments affected the mRNA level of TLR4, even though it plays a vital role in innate immunity (Fig. S3A†). However, the increased mRNA level of MyD88
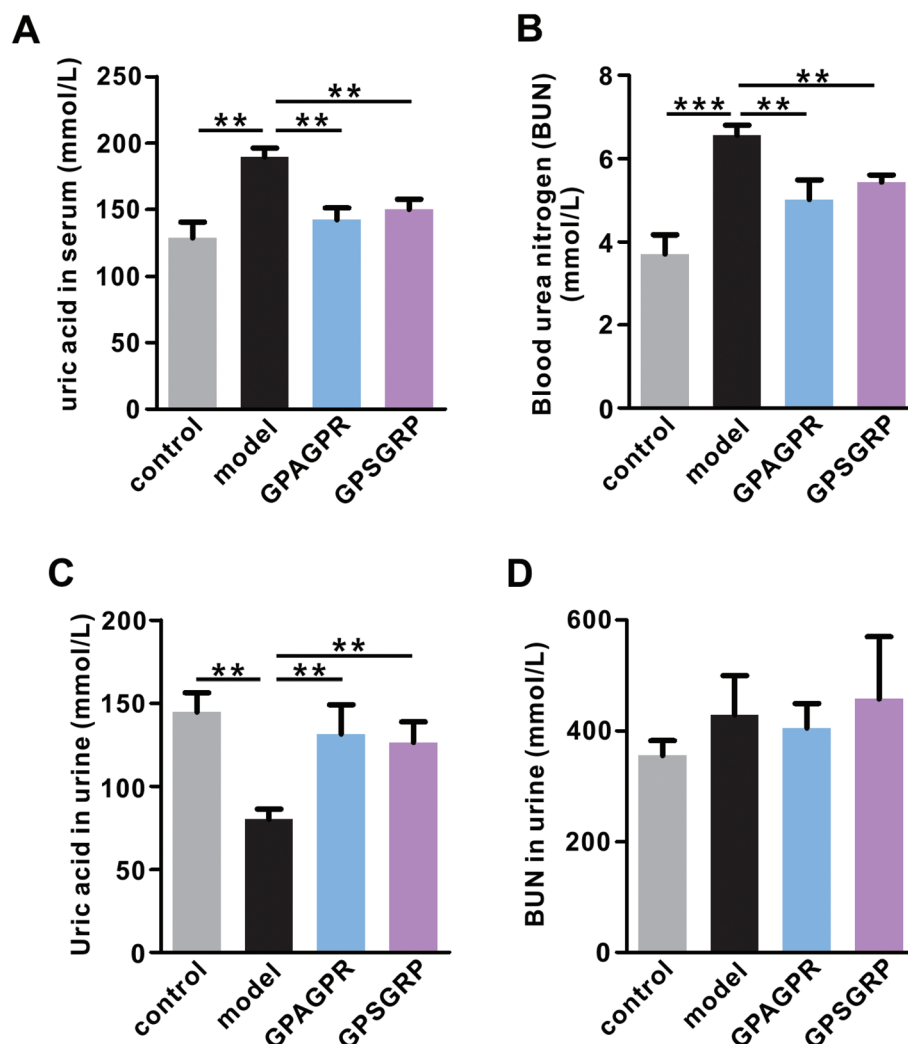
Fig. 2 The anti-HUA effects of GPAGPR and GPSGRP in mice. The concentrations of uric acid (A) and blood urea nitrogen (B) in serum. The concentrations of uric acid (C) and blood urea nitrogen (D) in urine. Data are shown as mean ± SD, n = 5. ** p < 0.01, and *** p < 0.001.

(p < 0.05), one of the key components related to TLR4 signal transduction, was further aggravated by the GPAGPR treatment (p < 0.01) but reduced by GPSGRP (p < 0.05) (Fig. S3B†). The mRNA level of iNOS, a factor downstream of the MyD88 signaling pathway, presented the same trend as the HUA phenotypes: HPD significantly upregulated the expression level of iNOS (p < 0.001), and the peptide treatments restored it to the control level (p < 0.01 and p < 0.05) (Fig. S3D†). However, constant mRNA levels of TRAF6 and COX-2 were observed among the groups (Fig. S3C and S3E†).

GPAGPR and GPSGRP treatments modulated the gut microbiota in HUA mice

After 12 weeks of treatment, cecal contents were collected and the extracted DNAs were sequenced to show the effects of HPD and peptide treatment on the gut microbiota. The reduced abundance (observed OTUs and Chao 1 index) of the gut microbiota induced by HPD was further aggravated by both peptide treatments, while the increased diversity (Shannon and Simpson indices) was restored (Fig. 5A). Weighted UniFrac PCoA showed that HPD shifted the overall structure of the gut microbiota away from the control group but the microbiota structure was subsequently altered by the peptide treatments. In addition, the GPAGPR and GPSGRP groups showed different structures, showing the different modulatory effects of these two peptides on the gut microbiota (Fig. 5B).

Six dominant phyla with more than 1% relative abundance were identified in this study, including Bacteroidetes, Firmicutes, Verrucomicrobia, Actinobacteria, Proteobacteria and Patescibacteria. HPD enhanced the abundance of the last five phyla and reduced the abundance of only Bacteroidetes. Both the GPAGPR and GPSGRP treatments aggravated the changes in the abundance of Bacteroidetes, Firmicutes and Patescibacteria and restored the abundance of Actinobacteria and Proteobacteria to the control levels, but Verrucomicrobia was restored by only GPSGRP (Fig. 5C and Table S4†). In addition, 15 genera with high abundance (>1% in at least one group) were shown in Fig. 5D and Table S5,† including
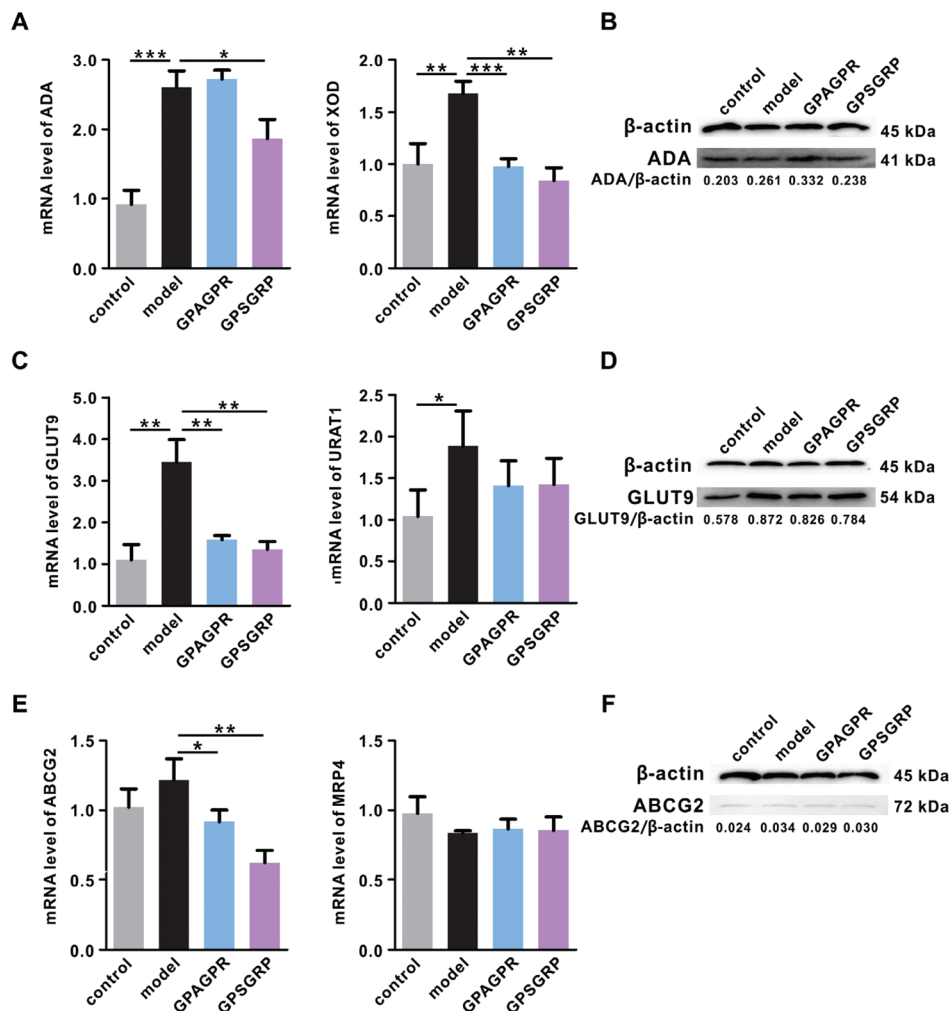
Fig. 3 Effects of GPAGPR and GPSGRP on the expression of genes involved in uric acid metabolism. A. mRNA levels of XOD and ADA in the liver. B. Protein level of ADA in the liver. C. mRNA levels of GLUT9 and URAT1 in the kidneys. D. Protein level of GLUT9 in the kidneys. E. mRNA levels of ABCG2 and MRP4 in the kidneys. F. Protein level of ABCG2 in the kidneys. Data are shown as mean ± SD, $n = 5$. * $p < 0.05$, ** $p < 0.01$, and *** $p < 0.001$.

Akkermansia, *Lactobacillus* and *Bifidobacterium*, which were well-known probiotics. Among these 15 genera, 8 and 9 genera were restored to control levels by GPAGPR and GPSGRP treatments, respectively, while only five genera were restored by both peptides. In addition, different change trends were observed in five genera, including *Akkermansia*, *Dubosiella*, *Alloprevotella*, *Clostridiales* unclassified and *Alistipes*. At the species level, 145 species were detected in all groups, while 25, 18, 35 and 24 species were identified in only the control, model, GPAGPR and GPSGRP groups, accounting for 10.7%, 7.6%, 14.8% and 10.6% of the total species in the four groups, respectively (Fig. 5E).

Forty-nine differentially abundant genera were identified by the Kruskal–Wallis test in this study (Fig. 5F and Table S6†). Among them, 23 and 28 genera were restored to the control level after GPAGPR and GPSGRP treatments, respectively, while 15 genera were restored by both peptides, which belonged to the phyla Actinobacteria ($n = 5$), Firmicutes ($n = 5$), Proteobacteria ($n = 3$), Tenericutes ($n = 1$) and Bacteroidetes ($n = 1$). In addition, Spearman's correlation analysis was carried out for these genera with phenotypes of HUA in serum and urine. Among them, 40 out of 49 genera were significantly correlated with at least one index, while only three genera, *Eggerthella*, *Ruminococcaceae* unclassified, and *Olsenella*, were significantly correlated with three indices.

GPAGPR and GPSGRP treatments altered the miRNA profile of the kidneys in HUA mice

Due to the relatively better XOD inhibition and HUA alleviation activity of GPSGRP, the miRNA profile of kidneys in HUA mice that received GPSGRP treatment was assessed. In total, 9 small RNA libraries were constructed, and 3 718 484 ± 1 271 019, 2 369 893 ± 174 885 and 2 800 077 ± 689 950 clean reads were generated from the control, model and GPSGRP groups, respectively (Table S7†). In total, 11 differentially expressed (DE) miRNAs (four upregulated and seven downregulated
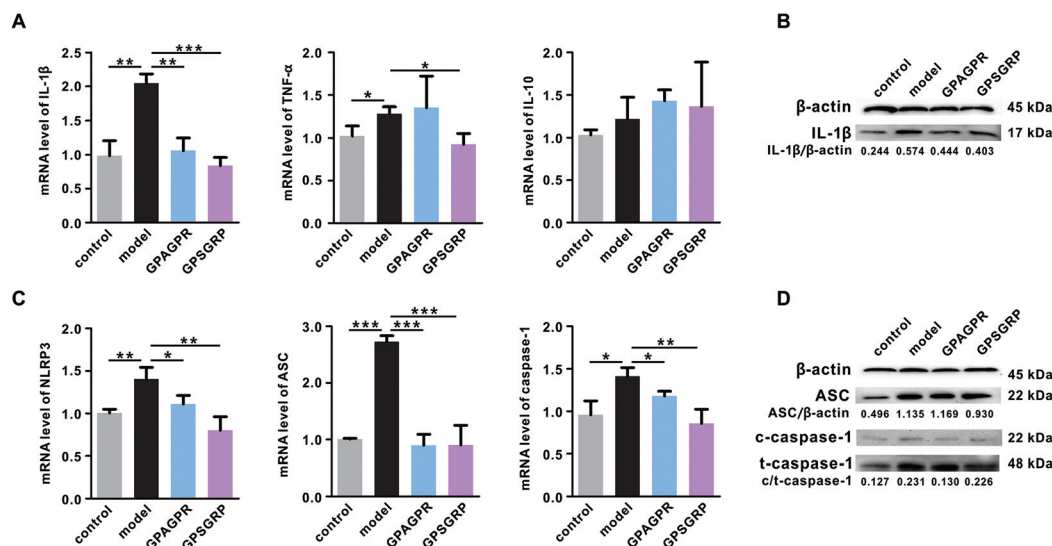
Fig. 4 Effects of GPAGPR and GPSGRP on the expression of genes involved in IL-1β release in the kidneys. A. mRNA levels of IL-1β, TNF-α and IL-10. B. Protein level of IL-1β. mRNA (C) and protein levels (D) of the NLRP3 inflammasome. Data are shown as mean ± SD, $n = 5$. * $p < 0.05$, ** $p < 0.01$, and *** $p < 0.001$.

miRNAs) were identified in the model group compared with that of the control group, while 13 DE-miRNAs (nine upregulated and four downregulated miRNAs) were identified in the peptide group compared with that of the model group (Fig. 6A). Twenty-one nonrepetitive and DE miRNAs were identified among the three groups in this study and the heatmap is shown in Fig. S4 and Table S8.† We sought to explore the role of these DE-miRNAs in regulating the expression of target genes and related functions. The putative target mRNAs of the DE-miRNAs were predicted and used for KEGG pathway analysis, and the top 10 significantly enriched KEGG pathways with the lowest p values were identified in the control and peptide groups when compared with those of the model group. Among them, four significantly enriched KEGG pathways were identified in both pairwise comparisons: microRNAs in cancer; pluripotency of stem cell regulation; the mTOR signaling pathway; and proteoglycans in cancer (Fig. 6B). In addition, the top five significantly enriched GO terms of the three categories in this study are shown in Fig. 6C. Among them, protein phosphorylation, and membrane and protein binding were the categories with the highest rich factor and lowest p value in terms of biological processes, cellular component and molecular function, respectively, in both pairwise comparisons.

In addition, 10 miRNAs (miR-143-3p, miR-34a, miR-223, miR-17-5p, miR-186, miR-125b-5p, miR-152-5p, miR-188-5p, miR-128-3p and miR-30b) were identified to be involved in uric acid metabolism, NLRP3 inflammasome, inflammation related signaling pathways and renal injury, and four of them (miR-125b-5p, miR-152-5p, miR-188-5p and miR-128-3p) were differentially expressed among groups (Tables S8 and S9†). Subsequently, spearman's correlation analysis was carried out for these 10 miRNAs with the abundance of 49 differentially

abundant genera. Among them, genus *Rikenellaceae RC9* was positively correlated (coefficient >0.95) with five miRNAs, while genera *Lactobacillus*, *Ruminococcaceae UCG-004*, *Eubacterium*, *Candidatus*, *Oligella*, *Pygmaiobacter*, *Oxyphotobacteria* unclassified, *Anaeroplasma*, *Escherichia*, *Shigella* and *Parasutterella* were correlated (coefficient >0.95 or <−0.95) with four miRNAs. On the other hand, miR-188-5p and miR-128-3p were correlated with 16 and 18 genera, respectively (Table S10†).

Discussion

Identification of peptides with distinct structures and functions and their subsequent use as biomarkers will contribute to the clarification of the underlying mechanism of peptides, the optimization of hydrolysis strategies and the improvement of hydrolysate product quality control. The AJOP mixture was previously reported to show beneficial effects on HUA.[7] In this study, two dominant peptides, GPAGPR and GPRGRP, were identified and investigated for their XOD inhibition and anti-HUA activities by the combination of *in silico*, *in vitro* and *in vivo* experiments, and their modulation effects on gene expression, gut microbiota and host miRNA profile were also explored.

The biological activities of peptides are related to their amino acid residue profiles. The XOD inhibitory activities of peptides are partly attributed to tryptophan (Trp) residues due to the similar C6 and C5 ring structures of Trp, allopurinol and xanthine,[22,28] while treatment with arginine (Arg) alone suppresses uric acid generation.[29] However, GPAGPR and GPSGRP contain one Arg each and no Trp but still showed XOD inhibitory activities (Fig. 1C–F). Both GPAGPR and GPSGRP are rich in Gly and Pro, but the presence of Gly and
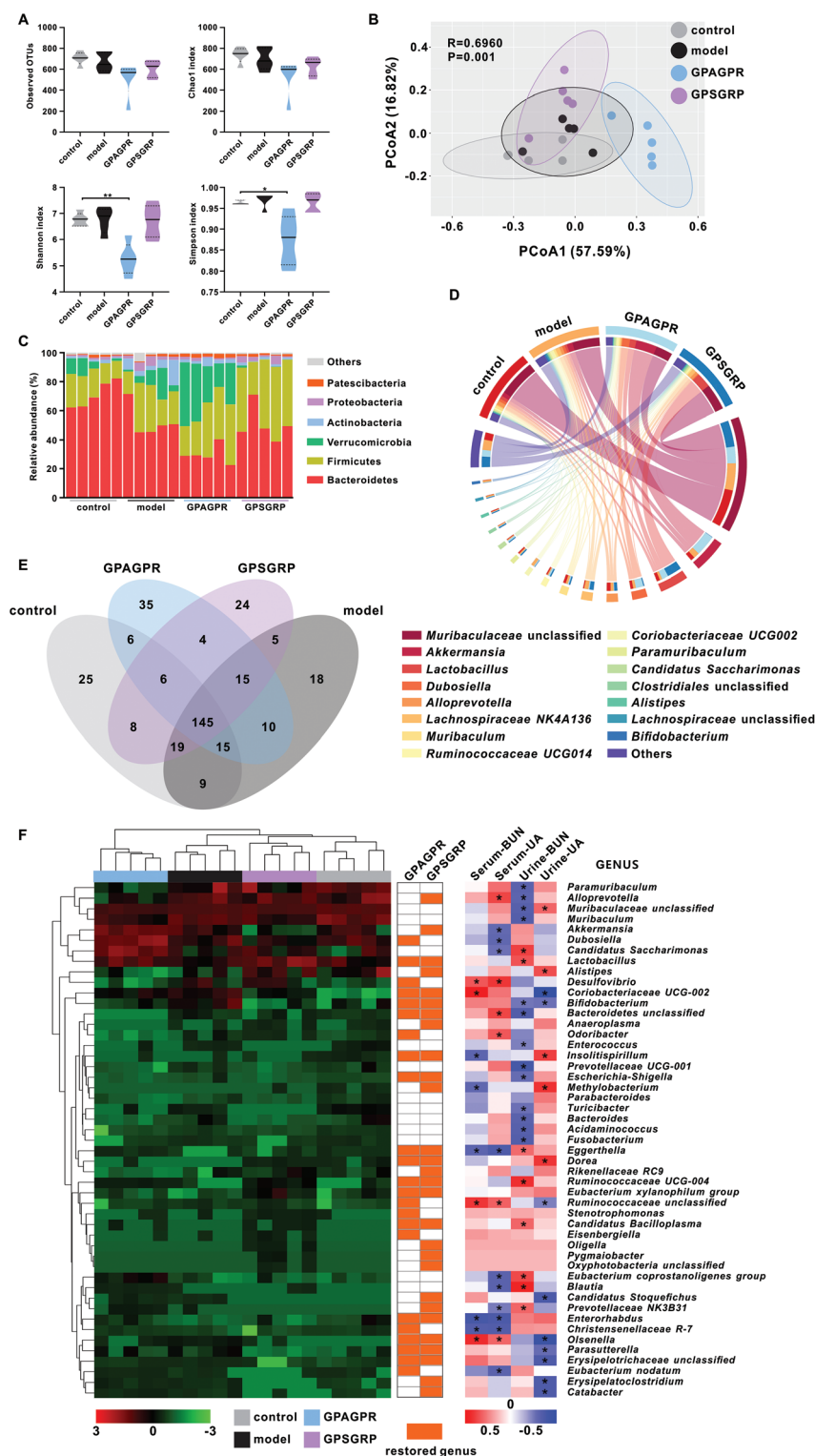
Fig. 5 Gut microbiota modulation in response to GPAGPR and GPSGRP in HUA mice. A. α diversity was assessed by observed OTUs and Chao1, Shannon and Simpson indices. B. Weighted UniFrac PCoA analysis of the gut microbiota. Dominant phyla (C) and genera (D) in each group. E. Distribution of species in each group examined *via* a Venn diagram. F. The relative abundance of differentially expressed genera and Spearman's correlation analysis of these genera with HUA phenotypes, including the concentrations of uric acid and blood urea nitrogen in serum and urine. The orange squares indicate that the abundance of the genus was restored by the peptide treatments. The heatmap on the left shows the abundance of genera, and the heatmap on the right shows the correlation coefficient value. Stars indicate a significant correlation (* $p < 0.05$).
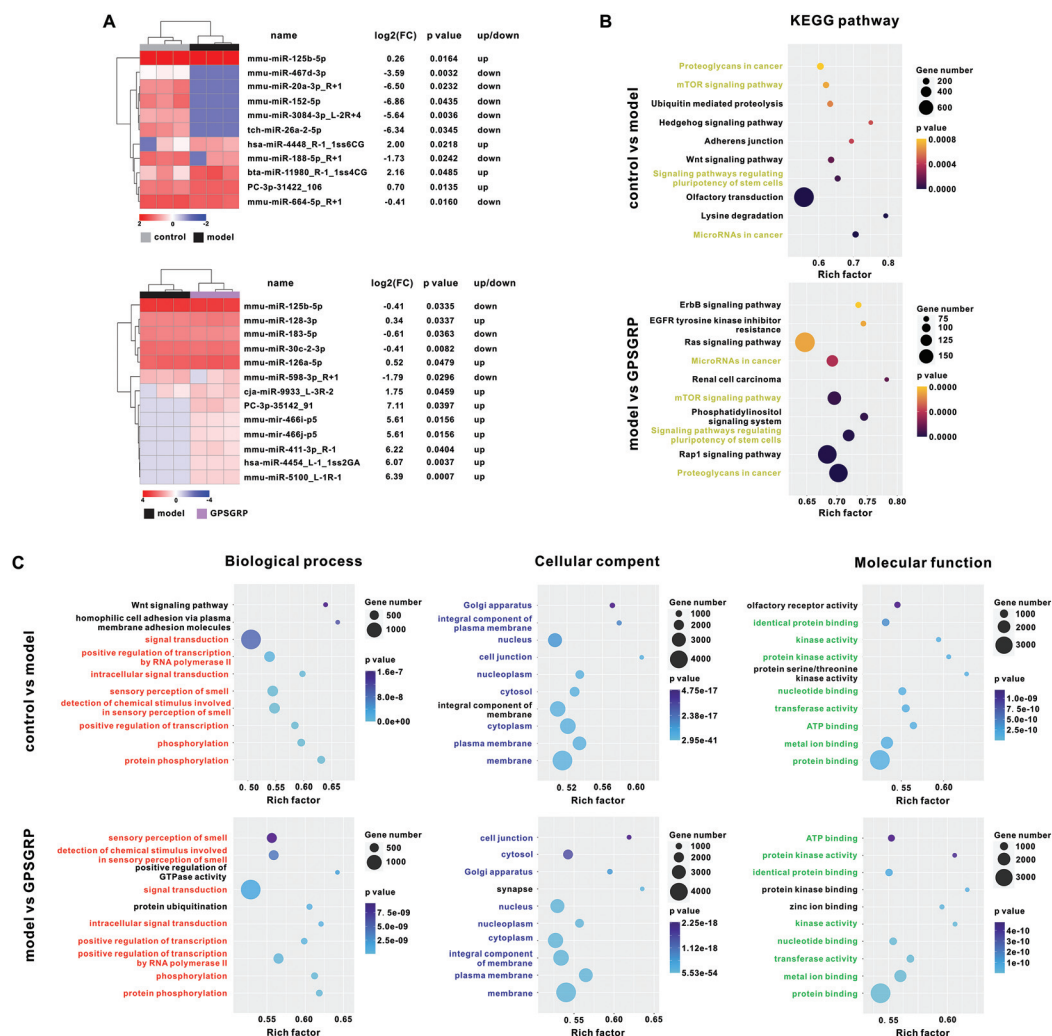
Fig. 6 Effects of GPSGRP treatment on the miRNA profile in HUA mice. A. DE miRNAs in the control and GPSGRP groups compared with the control group ($p < 0.05$). Top 10 enriched pathways (B) and GO terms (C) based on the predicted target genes of DE-miRNAs in two comparisons (control *vs.* model and model *vs.* GPSGRP).

Pro was reported to increase the availability of peptides that act as antioxidants instead of XOD inhibitors.[30] In fact, although XOD inhibition and antioxidation are different and independent processes, XOD inhibition is beneficial in most pathophysiological states due to the decrease in reactive oxygen species (ROS), which partly explains the antioxidant activity of allopurinol.[31] Therefore, we proposed that the amino acid residues related to antioxidant properties mainly contributed to the XOD inhibitory activity in these two peptides identified in this study.

GPAGPR and GPSGRP were predicted as XOD inhibitors *via* molecular docking and reduced the expression levels of XOD and inhibited uric acid biosynthesis in HUA mice, as expected (Fig. 3A and B). However, inhibited uric acid reabsorption, characterized by reduced mRNA and protein levels of GLUT9, was also observed in the peptide treatment group (Fig. 3C and D) although no interaction was predicted between GLUT9 and peptides. In this study, we proposed that the regulation of GLUT9 is mediated *via* miRNAs. miRNAs are noncoding RNA

molecules involved in the posttranscriptional regulation of gene expression by regulating mRNA degradation and/or binding to the 3′-UTR of target mRNAs to block protein translation, and they target more than 60% of protein coding genes in humans. As previously reported, miR-143-3p directly targets GLUT9 to reduce uric acid reabsorption at the cellular level,[16] and in this study, compared with the model group, the peptide treatment group showed increased miR-143-3p expression and decreased GLUT9 expression (Table S9†). Furthermore, miRNAs were reported to regulate multiple genes involved in inflammation. Studies have shown that the selective inhibition of the NF-κB pathway and NLRP3 inflammasome, which plays a vital role in generating pro-IL-1β and modifying pro-IL-1β to IL-1β, respectively, has renal protective effects.[4] In this study, the activation of the NLRP3 inflammasome and NF-κB pathway was inhibited by the peptide treatments, along with reduced IL-1β mRNA and protein expression levels (Fig. 3 and Fig. S1†). Notably, miRNA-223 directly targets the NLRP3 inflammasome,[18] while miR-17-5p regulates it indirectly by

binding and degrading the mRNA encoding thioredoxin-interacting protein.[32] Additionally, miR-186 showed inhibitory activity against the TLR4/NF-κB pathway in a mouse model.[33] In addition to regulating the related pathways, miR-488 and miR-920 were reported to directly target IL-1β.[34] All the related miRNAs except miR-488 and miR-920 were detected in this study, and the expected changing trend was found for miR-17-5p, which were downregulated in the model group and subsequently upregulated by the peptide treatments, while the expressions of miR-223 and miR-186 were only increased in the GPSGRP group compared to that of the model group (Table S9†). Additionally, most of the DE-miRNAs identified in this study were reported to be closely related to renal injury. Among them, miRNA-125b-5p and miR-152-5p were associated with renal injury and used as diagnostic biomarkers.[35,36] Furthermore, the interaction between miR-188-5p and PTEN was shown to regulate the PI3K/AKT signaling pathway and mediate diabetic kidney disease alleviation. MiR-128-3p directly targeted SIRT1 to induce kidney damage, and miR-30b participated in the onset of HUA by targeting the IL-6 receptor in mice.[37–39] However, the detected expression trends of some of the above-mentioned DE-miRNAs were not as expected (Table S9†), which might be due to the complicated network between miRNAs and mRNAs, and other target molecules of these DE-miRNAs might be involved in the alleviation of HUA and renal injury.

Previous studies reported the vital roles of the gut microbiota in HUA alleviation, and clarified that the anti-HUA effects of specific peptides or mixtures were mediated by the gut microbiota.[7,40,41] Firstly, genera *Escherichia* and *Proteus* were reported to promote uric acid formation by secreting XOD, while genera *Lactobacillus* and *Pseudomonas* inhibited purine absorption and degraded uric acid in the intestine.[14] In this study, the expected decrease in *Escherichia* and increase in *Lactobacillus* were detected in the two peptide treatment groups, with an extremely high abundance of the genus *Lactobacillus* in the GPSGRP group (21.49%), and both HPD and the peptide treatments showed no effect on the genus *Pseudomonas* (Table S6†). In addition, genera *Lactobacillus*, *Clostridium*, *Streptococcus*, *Akkermansia* and *Faecalibaculum* were known as SCFA producers,[42] and SCFAs were reported to provide energy for intestinal wall cells to excrete uric acid and alleviate HUA.[43] Among them, *Lactobacillus* and *Streptococcus* were increased by both peptide treatments, while the abundance of genus *Akkermansia*, also known as a potential next-generation probiotic, was increased by the HPD treatment (8.49%), further aggravated by GPAGPR (30.72%) but reduced by the GPSGRP treatment (0.36%) (Table S6†). Moreover, allopurinol, one of the most important clinical XOD inhibitors, was reported to modulate the gut microbiota by specifically decreasing the abundance of the genera *Adlercreutzia*, *Anaerostipes*, *Bilophila*, *Morganella* and *Desulfovibrio*.[44] Except for the undetected genus *Morganella* in this study, the GPAGPR and GPSGRP treatments decreased the abundance of two (*Bilophila* and *Desulfovibrio*) and three genera (*Bilophila*, *Adlercreutzia* and *Anaerostipes*) that allopurinol did, respect-

ively. However, it is not very clear whether these genera are closely related to the XOD inhibitory activity and anti-HUA effects.

In addition, metabolites derived from the gut microbiota are known as the potential regulators of miRNA expression. For example, tryptophan-derived metabolites (indole or its derivatives) were shown to negatively regulate miR-181 expression in adipocytes and alleviate obesity and insulin resistance; SCFAs were shown to control miRNA expression by regulating the DNA methylation or histone deacetylation of promoters and subsequently alleviate obesity and autoimmunity in the host; and bile acids were shown to increase the miR-92a-1-5p expression involved in the generation of an intestinal metaplasia phenotype from gastric cells by the FOXD1/NF-κB/CDX2 regulatory axis.[19–21,45] Among the 49 differentially abundant genera identified in this study, genera *Lactobacillus*, *Bifidobacterium* and *Enterococcus* catalyze the hydrolysis of conjugated BAs to preserve the metabolic balance of BA,[46] genera *Lactobacillus* and *Bifidobacterium* converted tryptophan to indole and its derivatives,[47] and genera *Lactobacillus*, *Akkermansia*, *Eubacterium* and *Blautia* generated SCFAs by the degradation of dietary fiber.[33] Spearman's correlation analysis indicated that both *Lactobacillus* and *Eubacterium* correlated with four miRNAs, and genera related to the metabolism of SCFAs, tryptophan and BA were totally correlated with 17, 7 and 12 miRNAs (Table S10†), proposing the vital roles of microbiota metabolites between the gut microbiota and miRNAs.

In conclusion, the peptides GPAGPR and GPSGRP screened from AJOP in this study exhibited XOD inhibitory activities and anti-HUA effects *in vitro* and *in vivo*. In addition, these peptides modulated the gut microbiota composition and altered the renal miRNA expression in the host, and we proposed that the microbiota-derived metabolites, including SCFAs, BAs and tryptophan derivatives, might act as links between miRNA and the gut microbiota, but the underlying mechanism needs to be further explored.

Author contributions

CYL and XRS designed this study. SQF, YMH, GDL, NS and RW carried out the experiments. SQF, YMH, NS, JJH, JZ, YL and CYL performed the data analysis. SQF, GDL, CYL, THM and LJD prepared the manuscript.

Conflicts of interest

All authors declare that they have no conflict of interest.

Acknowledgements

References

1 S. Hao, C. Zhang and H. Song, Natural products improving hyperuricemia with hepatorenal dual effects, *J. Evidence-Based Complementary Altern. Med.*, 2016, **2016**, 7390504.

2 R. Harrison, Structure and function of xanthine oxidoreductase: where are we now?, *Free Radical Biol. Med.*, 2002, **33**, 774–797.

3 H. Wan, J. Han, S. Tang, W. Bao, C. Lu, J. Zhou, T. Ming, Y. Li and X. Su, Comparisons of protective effects between two sea cucumber hydrolysates against diet induced hyperuricemia and renal inflammation in mice, *Food Funct.*, 2020, **11**, 1074–1086.

4 J. Tan, L. Wan, X. Chen, X. Li, X. Hao, J. Li and H. Ding, Conjugated linoleic acid ameliorates high fructose-induced hyperuricemia and renal inflammation in rats via NLRP3 inflammasome and TLR4 signaling pathway, *Mol. Nutr. Food Res.*, 2019, **63**, e1801402.

5 C. E. Ekpenyong and N. Daniel, Roles of diets and dietary factors in the pathogenesis, management and prevention of abnormal serum uric acid levels, *PharmaNutrition*, 2015, **3**, 29–45.

6 M. M. Ansari-Ramandi, M. Maleki, A. Alizadehasl, A. Amin, S. Taghavi, M. J. Alemzadeh-Ansari, A. Kazem Moussavi and N. Naderi, Safety and effect of high dose allopurinol in patients with severe left ventricular systolic dysfunction, *J. Cardiovasc. Thorac. Res.*, 2017, **9**, 102–107.

7 C. Lu, S. Tang, J. Han, S. Fan, Y. Huang, Z. Zhang, J. Zhou, T. Ming, Y. Li and X. Su, *Apostichopus japonicus* oligopeptide induced heterogeneity in the gastrointestinal tract microbiota and alleviated hyperuricemia in a microbiota-dependent manner, *Mol. Nutr. Food Res.*, 2021, **65**, e2100147.

8 J. Han, Z. Huang, S. Tang, C. Lu, H. Wan, J. Zhou, Y. Li, T. Ming, Z. Jim Wang and X. Su, The novel peptides ICRD and LCGEC screened from tuna roe show antioxidative activity via Keap1/Nrf2-ARE pathway regulation and gut microbiota modulation, *Food Chem.*, 2020, **327**, 127094.

9 A. T. Vieira, L. Macia, I. Galvão, F. S. Martins, M. C. Canesso, F. A. Amaral, C. C. Garcia, K. M. Maslowski, E. De Leon, D. Shim, J. R. Nicoli, J. L. Harper, M. M. Teixeira and C. R. Mackay, A role for gut microbiota and the metabolite-sensing receptor GPR43 in a murine model of gout, *Arthritis Rheumatol.*, 2015, **67**, 1646–1656.

10 Z. Guo, J. Zhang, Z. Wang, K. Y. Ang, S. Huang, Q. Hou, X. Su, J. Qiao, Y. Zheng, L. Wang, E. Koh, H. Danliang, J. Xu, Y. K. Lee and H. Zhang, Intestinal microbiota distinguish gout patients from healthy humans, *Sci. Rep.*, 2016, **6**, 20602.

11 T. Shao, L. Shao, H. Li, Z. Xie, Z. He and C. Wen, Combined signature of the fecal microbiome and metabolome in patients with gout, *Front. Microbiol.*, 2017, **8**, 268.

12 T. Koguchi and T. Tadokoro, Beneficial effect of dietary fiber on hyperuricemia in rats and humans: a review, *Int. J. Vitam. Nutr. Res.*, 2019, **89**, 89–108.

13 H. Wang, L. Mei, Y. Deng, Y. Liu, X. Wei, M. Liu, J. Zhou, H. Ma, P. Zheng, J. Yuan and M. Li, *Lactobacillus brevis* DM9218 ameliorates fructose-induced hyperuricemia through inosine degradation and manipulation of intestinal dysbiosis, *Nutrition*, 2019, **62**, 63–73.

14 J. Wang, Y. Chen, H. Zhong, F. Chen, J. Regenstein, X. Hu, L. Cai and F. Feng, The gut microbiota as a target to control hyperuricemia pathogenesis: Potential mechanisms and therapeutic strategies, *Crit. Rev. Food Sci. Nutr.*, 2021, 1–11, DOI: 10.1080/10408398.2021.1874287.

15 Y. T. Xu, Y. R. Leng, M. M. Liu, R. F. Dong, J. Bian, L. L. Yuan, J. G. Zhang, Y. Z. Xia and L. Y. Kong, MicroRNA and long noncoding RNA involvement in gout and prospects for treatment, *Int. Immunopharmacol.*, 2020, **87**, 106842.

16 Z. Zhou, Y. Dong, H. Zhou, J. Liu and W. Zhao, MiR-143-3p directly targets GLUT9 to reduce uric acid reabsorption and inflammatory response of renal tubular epithelial cells, *Biochem. Biophys. Res. Commun.*, 2019, **517**, 413–420.

17 W. F. Sun, M. M. Zhu, J. Li, X. X. Zhang, Y. W. Liu, X. R. Wu and Z. G. Liu, Effects of Xie-Zhuo-Chu-Bi-Fang on miR-34a and URAT1 and their relationship in hyperuricemic mice, *J. Ethnopharmacol.*, 2015, **161**, 163–169.

18 Q. B. Zhang, D. Zhu, F. Dai, Y. Q. Huang, J. X. Zheng, Y. P. Tang, Z. R. Dong, X. Liao and Y. F. Qing, MicroRNA-223 suppresses IL-1β and TNF-α production in gouty inflammation by targeting the NLRP3 inflammasome, *Front. Pharmacol.*, 2021, **12**, 637415.

19 H. N. Sanchez, J. B. Moroney, H. Gan, T. Shen, J. L. Im, T. Li, J. R. Taylor, H. Zan and P. Casali, B cell-intrinsic epigenetic modulation of antibody responses by dietary fiber-derived short-chain fatty acids, *Nat. Commun.*, 2020, **11**, 60.

20 A. T. Virtue, S. J. McCright, J. M. Wright, M. T. Jimenez, W. K. Mowel, J. J. Kotzin, L. Joannas, M. G. Basavappa, S. P. Spencer, M. L. Clark, S. H. Eisennagel, A. Williams, M. Levy, S. Manne, S. E. Henrickson, E. J. Wherry, C. A. Thaiss, E. Elinav and J. Henao-Mejia, The gut microbiota regulates white adipose tissue inflammation and obesity via a family of microRNAs, *Sci. Transl. Med.*, 2019, **11**(496), eaav1892, DOI: 10.1126/scitranslmed.aav1892.

21 T. Li, H. Guo, H. Li, Y. Jiang, K. Zhuang, C. Lei, J. Wu, H. Zhou, R. Zhu, X. Zhao, Y. Lu, C. Shi, Y. Nie, K. Wu, Z. Yuan, D. M. Fan and Y. Shi, MicroRNA-92a-1-5p increases CDX2 by targeting FOXD1 in bile acids-induced gastric intestinal metaplasia, *Gut*, 2019, **68**, 1751–1763.

22 C. Hou, D. Liu, M. Wang, C. Gong, Y. Li, L. Yang, M. Yao, E. Yuan and J. Ren, Novel xanthine oxidase-based cell model using HK-2 cell for screening antihyperuricemic functional compounds, *Free Radical Biol. Med.*, 2019, **136**, 135–145.

23 N. Liu, Y. Wang, M. Yang, W. Bian, L. Zeng, S. Yin, Z. Xiong, Y. Hu, S. Wang, B. Meng, J. Sun and X. Yang, New rice-derived short peptide potently alleviated hyperuricemia induced by potassium oxonate in rats, *J. Agric. Food Chem.*, 2019, **67**, 220–228.

24 S. Reagan-Shaw, M. Nihal and N. Ahmad, Dose translation from animal to human studies revisited, *FASEB J.*, 2008, **22**, 659–661.

25 C. C. Wang, L. Du, H. H. Shi, L. Ding, T. Yanagita, C. H. Xue, Y. M. Wang and T. T. Zhang, Dietary EPA-enriched phospholipids alleviate chronic stress and LPS-induced depression- and anxiety-like behavior by regulating immunity and neuroinflammation, *Mol. Nutr. Food Res.*, 2021, **65**, e2100009.

26 C. Lu, T. Sun, Y. Li, D. Zhang, J. Zhou and X. Su, Modulation of the gut microbiota by krill oil in mice fed a high-sugar high-fat diet, *Front. Microbiol.*, 2017, **8**, 905.

27 P. D. Schloss, S. L. Westcott, T. Ryabin, J. R. Hall, M. Hartmann, E. B. Hollister, R. A. Lesniewski, B. B. Oakley, D. H. Parks, C. J. Robinson, J. W. Sahl, B. Stres, G. G. Thallinger, D. J. Van Horn and C. F. Weber, Introducing mothur: open-source, platform-independent, community-supported software for describing and comparing microbial communities, *Appl. Environ. Microbiol.*, 2009, **75**, 7537–7541.

28 A. B. Nongonierma and R. J. Fitzgerald, Tryptophan-containing milk protein-derived dipeptides inhibit xanthine oxidase, *Peptides*, 2012, **37**, 263–272.

29 W. A. Saka, R. E. Akhigbe, A. O. Abidoye, O. S. Dare and A. O. Adekunle, Suppression of uric acid generation and blockade of glutathione dysregulation by L-arginine ameliorates dichlorvos-induced oxidative hepatorenal damage in rats, *Biomed. Pharmacother.*, 2021, **138**, 111443.

30 A. Alemán, B. Giménez, E. Pérez-Santin, M. C. Gomez-Guillen and P. Montero, Contribution of Leu and Hyp residues to antioxidant and ACE-inhibitory activities of peptide sequences isolated from squid gelatin hydrolysate, *Food Chem.*, 2012, **125**, 334–341.

31 J. Luo, D. Yan, S. Li, S. Liu, F. Zeng, C. W. Cheung, H. Liu, M. G. Irwin, H. Huang and Z. Xia, Allopurinol reduces oxidative stress and activates Nrf2/p62 to attenuate diabetic cardiomyopathy in rats, *J. Cell. Mol. Med.*, 2020, **24**, 1760–1773.

32 D. Chen, B. J. Dixon, D. M. Doycheva, B. Li, Y. Zhang, Q. Hu, Y. He, Z. Guo, D. Nowrangi, J. Flores, V. Filippov, J. H. Zhang and J. Tang, IRE1α inhibition decreased TXNIP/NLRP3 inflammasome activation through miR-17–5p after neonatal hypoxic-ischemic brain injury in rats, *J. Neuroinflammation*, 2018, **15**, 32.

33 Y. Zhang, L. Ma, E. Lu and W. Huang, Atorvastatin upregulates microRNA-186 and inhibits the TLR4-mediated MAPKs/NF-κB pathway to relieve steroid-induced avascular necrosis of the femoral head, *Front. Pharmacol.*, 2021, **12**, 583975.

34 W. Zhou, Y. Wang, R. Wu, Y. He, Q. Su and G. Shi, MicroRNA-488 and -920 regulate the production of proinflammatory cytokines in acute gouty arthritis, *Arthritis Res. Ther.*, 2017, **19**, 203.

35 A. Duan, L. Liu, Y. Lou, D. Zhang, H. Li, Y. Chen, W. Cui and L. Miao, Diagnostic Value of Urinary miR-152–5p in Patients with IgA Nephropathy with Elevated Proteinuria Levels., *Clin. Lab.*, 2019, **65**(7), DOI: 10.7754/Clin.Lab.2019.190111.

36 S. Wang, L. Wu, L. Du, H. Lu, B. Chen and Y. Bai, Reduction in miRNA-125b-5p levels is associated with obstructive renal injury, *Biomed. Rep.*, 2017, **6**, 449–454.

37 M. Xue, Y. Cheng, F. Han, Y. Chang, Y. Yang, X. Li, L. Chen, Y. Lu and B. Sun, Triptolide attenuates renal tubular epithelial-mesenchymal transition via the MiR-188–5p-mediated PI3K/AKT pathway in diabetic kidney disease, *Int. J. Biol. Sci.*, 2018, **14**, 1545–1557.

38 T. Ye, X. Yang, H. Liu, P. Lv, H. Lu, K. Jiang, E. Peng, Z. Ye, Z. Chen and K. Tang, Theaflavin protects against oxalate calcium-induced kidney oxidative stress injury via upregulation of SIRT1, *Int. J. Biol. Sci.*, 2021, **17**, 1050–1060.

39 X. Zhong, Y. Chen, C. Yao, L. Xu, Y. Peng, Q. Yang, M. Zhao and X. Guo, MicroRNA-30b participates in the pathological process of hyperuricemia by regulating interleukin-6 receptor, *Nucleosides, Nucleotides Nucleic Acids*, 2020, **39**, 1162–1178.

40 J. Han, X. Wang, S. Tang, C. Lu, H. Wan, J. Zhou, Y. Li, T. Ming, Z. J. Wang and X. Su, Protective effects of tuna meat oligopeptides (TMOP) supplementation on hyperuricemia and associated renal inflammation mediated by gut microbiota, *FASEB J.*, 2020, **34**, 5061–5076.

41 J. Han, Z. Wang, C. Lu, J. Zhou, Y. Li, T. Ming, Z. Zhang, Z. J. Wang and X. Su, The gut microbiota mediates the protective effects of anserine supplementation on hyperuricaemia and associated renal inflammation, *Food Funct.*, 2021, **12**, 9030–9042.

42 L. Zhao, F. Zhang, X. Ding, G. Wu, Y. Y. Lam, X. Wang, H. Fu, X. Xue, C. Lu, J. Ma, L. Yu, C. Xu, Z. Ren, Y. Xu, S. Xu, H. Shen, X. Zhu, Y. Shi, Q. Shen, W. Dong, R. Liu, Y. Ling, Y. Zeng, Q. Zhang, J. Wang, L. Wang, Y. Wu, B. Zeng, H. Wei, M. Zhang, Y. Peng and C. Zhang, Gut bacteria selectively promoted by dietary fibers alleviate type 2 diabetes, *Science*, 2018, **359**, 1151–1156.

43 M. Nieuwdorp, P. W. Gilijamse, N. Pai and L. M. Kaplan, Role of the microbiome in energy regulation and metabolism, *Gastroenterology*, 2014, **146**, 1525–1533.

44 Y. Yu, Q. Liu, H. Li, C. Wen and Z. He, Alterations of the gut microbiome associated with the treatment of hyperuricaemia in male rats, *Front. Microbiol.*, 2018, **9**, 2233.

45 J. Du, P. Zhang, J. Luo, L. Shen, S. Zhang, H. Gu, J. He, L. Wang, X. Zhao, M. Gan, L. Yang, L. Niu, Y. Zhao, Q. Tang, G. Tang, D. Jiang, Y. Jiang, M. Li, A. Jiang, L. Jin, J. Ma, S. Shuai, L. Bai, J. Wang, B. Zeng, D. Wu, X. Li and

L. Zhu, Dietary betaine prevents obesity through gut microbiota-derived microRNA-378a family, *Gut Microbes*, 2021, **13**, 1–19.

46 Z. Song, Y. Cai, X. Lao, X. Wang, X. Lin, Y. Cui, P. K. Kalavagunta, J. Liao, L. Jin, J. Shang and J. Li,

Taxonomic profiling and populational patterns of bacterial bile salt hydrolase (BSH) genes based on worldwide human gut microbiome, *Microbiome*, 2019, **7**, 9.

47 H. M. Roager and T. R. Licht, Microbial tryptophan catabolites in health and disease, *Nat. Commun.*, 2018, **9**, 3294.

This journal is © The Royal Society of Chemistry 2022